Pflügers Archiv - European Journal of Physiology (2020) 472:103–115
https://doi.org/10.1007/s00424-019-02331-x

MUSCLE PHYSIOLOGY

The functional association between the sodium/bicarbonate cotransporter (NBC) and the soluble adenylyl cyclase (sAC) modulates cardiac contractility

María S. Espejo[1] · Alejandro Orlowski[1] · Alejandro M. Ibañez[1] · Romina A. Di Mattía[1] · Fernanda Carrizo Velásquez[1] · Noelia S. Rossetti[1] · María C. Ciancio[1] · Verónica C. De Giusti[1] · Ernesto A. Aiello[1]

Received: 26 June 2019 / Revised: 15 October 2019 / Accepted: 13 November 2019 / Published online: 22 November 2019

Abstract

The soluble adenylyl cyclase (sAC) was identified in the heart as another source of cyclic AMP (cAMP). However, its cardiac physiological function is unknown. On the other hand, the cardiac Na^+/HCO_3^- cotransporter (NBC) promotes the cellular co-influx of HCO_3^- and Na^+. Since sAC activity is regulated by HCO_3^-, our purpose was to investigate the potential functional relationship between NBC and sAC in the cardiomyocyte. Rat ventricular myocytes were loaded with Fura-2, Fluo-3, or BCECF to measure Ca^{2+} transient (Ca^{2+}_i) by epifluorescence, Ca^{2+} sparks frequency (CaSF) by confocal microscopy, or intracellular pH (pH_i) by epifluorescence, respectively. Sarcomere or cell shortening was measured with a video camera as an index of contractility. The NBC blocker S0859 (10 μM), the selective inhibitor of sAC KH7 (1 μM), and the PKA inhibitor H89 (0.1 μM) induced a negative inotropic effect which was associated with a decrease in Ca^{2+}_i. Since PKA increases Ca^{2+} release through sarcoplasmic reticulum RyR channels, CaSF was measured as an index of RyR open probability. The generation of CaSF was prevented by KH7. Finally, we investigated the potential role of sAC activation on NBC activity. NBC-mediated recovery from acidosis was faster in the presence of KH7 or H89, suggesting that the pathway sAC-PKA is negatively regulating NBC function, consistent with a negative feedback modulation of the HCO_3^- influx that activates sAC. In summary, the results demonstrated that the complex NBC-sAC-PKA plays a relevant role in Ca^{2+} handling and basal cardiac contractility.

Keywords cAMP · Cardiac myocytes · Sodium/bicarbonate cotransporter · Soluble adenylyl cyclase

Introduction

Historically, the only known source of cAMP in mammals was a family of hormone-responsive, transmembrane adenylyl cyclases (tmACs). However, in 1975 the activity of a Mn^{2+}-sensitive adenylyl cyclase localized in the cytosol (sAC) was described for the first time [7]. In 1999, the group of Levin and Buck purified and cloned the protein from rat testis [8]. It is known today that sAC has a wide distribution throughout the body, including the kidney [21], eye [37], gastrointestinal tract [20, 39], lung [3, 44], pancreas [52], bone [18], nervous system [22], and heart [2, 33, 45]. Additionally, it was demonstrated that sAC was not only present soluble in the cytoplasm but also found in discrete locations such as the nucleus, mitochondria, centrioles, or cilia [34, 38, 51].

sAC represents a possible alternative source of cAMP that is not limited to the plasma membrane, thus permitting the generation of cAMP proximal to intracellular targets and generating discrete signaling microdomains that provides both, specificity and selectivity [51]. sAC is directly regulated by bicarbonate ions (HCO_3^-) [11, 24]. HCO_3^- induces an allosteric change that increases the Vmax of sAC without changing its Km for substrate ATP [35]. Importantly, for mammalian sAC, HCO_3^- half-maximal effect (EC50) ranges between

María S. Espejo and Alejandro Orlowski contributed equally to the manuscript.

✉ Verónica C. De Giusti
degiustiveronica@gmail.com

✉ Ernesto A. Aiello
aaiello@ciclaplata.org.ar

[1] Centro de Investigaciones Cardiovasculares, Facultad de Ciencias Médicas, Universidad Nacional de La Plata-CONICET, Calle 60 y 120, 1900 La Plata, Argentina

10 and 25 mM [11, 26], which is approximately equivalent to the [HCO_3^-] levels found inside the cells and in plasma. Interestingly, it has been proposed that sAC might act as an intracellular sensor of pH/HCO_3^- [32]. Fortunately, in 2013 a specific inhibitor of sAC called KH7 was described [6] becoming the most helpful pharmacological tool to study the effects of this enzyme.

In the heart, cAMP is associated with the modulation of the excitation-contraction coupling (ECC). cAMP transduces signals to intracellular effectors including cAMP-dependent protein kinase (PKA), guanine exchange factors (i.e., exchange proteins activated by cAMP, EPACs), and cyclic nucleotide-gated channels [5, 15]. PKA phosphorylates several proteins involved in the ECC: voltage-gated L-type Ca^{2+} channels (Ca_L), sarcoplasmic reticulum (SR) Ca^{2+} release channels (or ryanodine receptor, RyR) [4, 46], sarcomeric proteins as troponin I (TnI) [36] and myosin binding protein C (MBP-C) [17] and phospholamban (PLB) [19]. PKA modifies contractility mainly by the phosphorylation of Ca_L and RyRs, leading to increased Ca^{2+} current (I_{Ca}) combined with greater availability of Ca^{2+} from the SR. Besides, phosphorylation of PLB blocks the inhibitory effect that this protein exerts on the SR Ca^{2+} ATPase (SERCA-2A) pump, leading to more efficient Ca^{2+} re-uptake in the SR.

An important mechanism for the entry of HCO_3^- in cardiac myocytes is the sodium/bicarbonate cotransporter (NBC), which introduces HCO_3^- and Na^+, and therefore, alkalinize the cell [13, 40, 41, 48, 49]. At least two isoforms of NBC exist in the heart, the electroneutral (NBCn1: $1HCO_3^-/1Na^+$) and the electrogenic (NBCe1: $2HCO_3^-/1Na^+$) [13]. In physiological conditions, both isoforms exhibit an equivalent activity for the maintenance of intracellular pH (pH_i) [13, 28], sharing this task with the Na^+/H^+ exchanger (NHE) [40, 41]. As sAC generates a small and constant amount of cAMP and it is primarily regulated by HCO_3^-, we hypothesized that the functional complex formed by NBC-sAC might be important for the regulation of basal cardiac contractility. Evidence validating this hypothesis is given in the present work.

Material and methods

All experiments were performed following the Guide for the Care and Use of Laboratory Animals (NIH Publication No. 85-23, revised 1996) and approved by the Institutional Animal Care and Use Committee of La Plata University.

Myocytes isolation

Male Wistar rat cardiomyocytes were isolated according to the technique previously described with some modifications [28]. Briefly, the hearts were attached via the aorta to a cannula, excised, and mounted on a Langendorff apparatus. They were then retrograde perfused at 37 °C at a constant perfusion pressure of 70–80 mmHg with Krebs-Henseleit solution (K-H) of the following composition (in mM): 146.2 NaCl, 4.7 KCl, 1 $CaCl_2$, 10 HEPES, 0.35 NaH_2PO_4, 1 $MgSO_4$, and 10 glucose (pH adjusted to 7.4 with NaOH). The solution was continuously bubbled with 100% O_2. After a stabilization period of 4 min, the perfusion was switched to a nominally Ca^{2+}-free K-H for 5 min. Hearts were then recirculated with collagenase (180 units/ml) and 1% BSA in K-H containing 50 μM $CaCl_2$. Perfusion continued until hearts became flaccid (15–25 min). Hearts were then removed from the perfusion apparatus by cutting at the atrioventricular junction. The desegregated myocytes were separated from the undigested tissue and rinsed several times with a K-H solution with increasing concentrations of $CaCl_2$ (from 50 μM to 1 mM). After each wash, myocytes were left for sedimentation for 10 min. Myocytes were kept in K-H solution (1 mM $CaCl_2$) at room temperature (20–22 °C) until use when they were changed to a HCO_3^- solution bubbling with 5% CO_2 and 95% O_2. Only rod-shaped ventricular myocytes with clear and distinct striations and an obvious marked shortening and relaxation on stimulation were used. Experiments were performed at room temperature.

Sarcomere and cell shortening

In order to measure sarcomere length (SL) or cell length (CL), myocytes were placed in a perfusion chamber on the stage of an inverted microscope (Nikon TE2000-U) and continuously superfused with a solution containing (mM) 5 KCl, 118 NaCl, 1.2 $MgSO_4$, 0.8 $MgCl_2$, 1 $CaCl_2$, 10 glucose, and 20 $NaHCO_3$, pH 7.4 after continuous bubbling with 5% CO_2 and 95% O_2 (HCO_3^- solution). The myocytes were stimulated via two platinum electrodes on either side of the bath at 0.5 Hz. SL and CL were recorded using specific software (IonWizard analysis software). The myocytes were observed using a video camera connected to the microscope. A determined region of the myocyte or the cell borders were measured for recording SL and CL, respectively. In the case of SL, the software estimated the most frequent length in that region using fast Fourier transform analysis (IonOptix, Milton, MA). The experiments were performed at room temperature.

Calcium transient

Sarcomere shortening and Fura-2 fluorescence were measured simultaneously. Myocytes were loaded with 2 μM Fura-2, AM (Thermo Fisher) for 10 min. Fura-2 fluorescence was measured on an inverted microscope adapted for epifluorescence with an IonOptix hardware. Cells were continuously superfused with HCO_3^--buffered solution (pH 7.4) at a constant flow of 1 ml/min and field stimulated at 0.5 Hz via two platinum electrodes on either side of the bath. The ratio of the Fura-2 fluorescence obtained after exciting the dye at 340 and 380 nm was taken as an index of the changes

in Ca^{2+} during paced experiments. Time to 50% relaxation was used as a parameter of the rate of Ca^{2+} decay. For SR Ca^{2+} content measurement, a solution containing 10 mM caffeine was rapidly applied onto cells. The amplitude of the caffeine-induced Ca^{2+} transient was used to estimate sarcoplasmic reticulum Ca^{2+} content.

Detection of spontaneous Ca^{2+} release (Ca^{2+} sparks) by confocal microscopy

Myocytes were loaded with 3 μM Fluo-3, AM (Thermo Fisher) and mounted on a Zeiss 410 inverted confocal microscope (LSMTech, Pennsylvania, USA). Cells were imaged in line scan mode along their long axis and avoiding the nucleus. Loaded cardiomyocytes were excited with the 488-nm line of an argon laser and emission at > 515 nm was collected. The images of Ca^{2+} sparks in time were registered in quiescent cardiac myocytes immediately after being paced. Data images were analyzed using "Sparkmaster," a plugin for ImageJ software [31].

pH_i measurements

pH_i was measured in single myocytes with an epifluorescence system (IonOptix, Milton, MA). Myocytes were incubated at room temperature for 10 min with 3 μM BCECF, AM (Thermo Fisher) followed by 15 min of washout. Dye-loaded cells were placed in a chamber on the stage of an inverted microscope (Nikon TE2000-U) and continuously superfused with a solution containing (mM) 5 KCl, 118 NaCl, 1.2 $MgSO_4$, 0.8 Cl_2Mg, 1.35 Cl_2Ca, 10 glucose, and 20 $NaHCO_3$, pH 7.4 after continuous bubbling with 5% CO_2 and 95% O_2. The myocytes were stimulated via two platinum electrodes on either side of the bath at 0.5 Hz. Dual excitation (440 and 495 nm) was provided by a 75-W xenon arc lamp and transmitted to the myocytes. Emitted fluorescence was collected with a photomultiplier tube equipped with a band-pass filter centered at 535 nm. The 495-to-440 nm fluorescence ratio was digitized at 10 kHz (IonWizard fluorescence analysis software). At the end of each experiment, the fluorescence ratio was converted to pH by in vivo calibrations using the high K^+-nigericin method [30]. The experiments were performed in HCO_3^--buffered solution.

Ammonium pulses

In order to examine the NBC activity in isolation, all the experiments were performed in the presence of 10 μM cariporide (HOE642, NHE blocker). The total NBC activity was assessed by evaluating the pH_i recovery from a double ammonium pre-pulse (the first acting as a control for the second pulse) [12]. KH7 (sAC inhibitor) or H89 (PKA inhibitor) was added 10 min before the beginning of the second ammonium pulse and was present throughout the rest of the experiment. The dpH_i/dt at each pH_i, obtained from an exponential fit of the recovery phase, was analyzed to calculate the net HCO_3^- influx (J_{HCO3-}), then $J_{HCO3-} = \beta_{tot}\, dpH_i/dt$, where β_{tot} is total intracellular buffering capacity. β_{tot} was calculated by the sum of the intracellular buffering due to CO_2 (β_{CO2}) plus the intrinsic buffering capacity (β_i). β_{CO2} was calculated as $\beta_{CO2} = 2.3\,[HCO_3^-]_i$, where $[HCO_3^-]_i = [HCO_3^-]_o\, 10^{pHi-pHo}$ [12]. β_i of the myocytes was measured by exposing cells to varying concentrations of NH_4Cl in Na^+-free HEPES bathing solution. pH_i was allowed to stabilize in Na^+-free solution before the application of NH_4Cl. β_i was calculated from the equation $\beta_i = \Delta[NH_4^+]_i/\Delta pH_i$ and referred to the mid-point values of the measured changes in pH_i. β_i at different levels of pH_i was estimated from the least-squares regression lines β_i vs. pH_i plots [12].

Subcellular fractioning and western blotting

Cytosolic fraction All the steps of the subcellular fractioning were done at 4 °C. Pericardium was removed and hearts were placed in A buffer containing mannitol 270 mM and Tris-HCl 10 mM at pH 7.4. After both atria and right ventricle were removed, the remaining left ventricle was homogenized manually with a Dounce homogenizer in A buffer at 20% [w/v]. The suspension was centrifuged at 800×*g* for 10 min. The supernatant was centrifuged again at 9000×*g* for 20 min, the pellet was enriched with mitochondria and discarded. The second supernatant was further centrifuged at 105,000×*g* for an hour to obtain the cytosolic fraction at the supernatant.

Mitochondrial fraction All the steps of the subcellular fractioning were done at 4 °C. The hearts were rapidly excised and placed in an ice-cold isolation buffer (IS) containing 75 mM sucrose, 225 mM mannitol, 1 mM EGTA, and 10 mM Tris, at pH 7.4. After both atria and right ventricle were removed, the remaining left ventricle was homogenized manually with a Dounce homogenizer in the presence of proteinase Type XXIV (0.8 mg in 5 ml of IS, P8038; Sigma). Homogenized tissue was centrifuged 5 min at 480×*g*, and the pellet containing unbroken cells and nuclei was discarded. The resulting supernatant containing the mitochondrial fraction was further centrifuged at 7700×*g* for 10 min and the supernatant was discarded. Then, the pellet was re-suspended in IS buffer and further centrifuged at 7700×*g* (3 × 5 min), and the final pellet was re-suspended in IB containing 75 mM sucrose, 225 mM mannitol, and 1 M Tris, at pH 7.4.

Testis was homogenized in RIPA lysis buffer with inhibitor protease cocktail at 20% [w/v]. After centrifugation of 20,000×*g* for 10 min at 4 °C, the supernatant was used for protein concentration determinations.

Protein concentration of mitochondrial and cytosolic fractions and testis homogenates was determined by the Bradford method. Samples were prepared by addition of SDS-PAGE

sample buffer (20% [v/v] glycerol, 2% [v/v] 2-mercaptoethanol, 4% [w/v] SDS, 1% [w/v] bromophenol blue, 150 mM Tris, pH 6.8) and 150 μg of protein. Samples were resolved by SDS-PAGE on 8% Laemmli acrylamide gels. Proteins were transferred to polyvinylidene difluoride membranes by electrophoresis for an hour at 100 V at room temperature in buffer composed of 20% (v/v) ethanol, Tris 25 mM, and glycine 192 mM. Polyvinylidene difluoride membranes were then blocked by incubation for 2 h in T-TBS buffer (0.1% (v/v) Tween-20, NaCl 137 mM, Tris 20 mM, pH 7.5), containing 5% (w/v) nonfat dry milk, and then incubated overnight with the corresponding primary antibodies: monoclonal mouse anti-sAC (CEP-Biotech, cat#R21.002), monoclonal mouse anti-GAPDH (Santa Cruz Biotechnology, a cytosolic protein marker), and polyclonal rabbit anti-VDAC (Sigma, a mitochondrial protein marker). Peroxidase-conjugated anti-rabbit (Santa Cruz) and anti-mouse (Invitrogen) were used as secondary antibodies. Bands were visualized with enhanced chemiluminescence reagent (ECL, Millipore) in a Chemidoc Station (Bio-Rad).

Chemicals

All drugs used in the present study were of analytical reagent and the concentrations used were selected according to previous reports; KH7 (1 μM), H89 (0.1 μM), and H3131 (5 μM) were purchased from Sigma–Aldrich. HOE 642 (10 μM) and S0859 (10 μM) were kindly donated by Sanofi-Aventis.

Statistical analysis

Unpaired or paired Student's *t* test or one-way ANOVA was used for statistical comparisons when appropriate. Data are expressed as mean ± SEM. Differences were considered significant at $p < 0.05$. All analyses were made using GraphPad Prism 6.0 (GraphPad Software, USA).

Results

Role of sAC in basal cardiac contractility

It is well known that the β-adrenergic stimulus activates the tmACs, generating cAMP, which finally increases PKA activity. In the heart, PKA is involved in the regulation of the proteins that participate in ECC, increasing cardiac contraction in response to an adrenergic stimulus. Since it has been demonstrated that sAC is able to generate cAMP in basal conditions (independent of an adrenergic activation) in different cell types and tissues, this mechanism might be able to regulate basal cardiac contractility. In order to evaluate this possibility, we treated the myocytes with the selective sAC blocker, KH7 (1 μM). Figure 1 shows that in the presence of KH7 the myocytes exert a negative inotropic effect (NIE) of approximately 20%, suggesting that sAC is involved in the normal generation of basal cardiac contractility. In addition, we used another sAC inhibitor called 2-hidroxiestradiol (H3131, 5 μM), and we obtained similar results (% of sarcomere shortening; control: 15.49 ± 1.49% vs. H3131: 12.71 ± 1.65%; $n = 5$, $p < 0.05$).

Role of HCO_3^- in basal cardiac contractility

As it has been demonstrated that sAC is stimulated by HCO_3^-, we hypothesized that the sAC-dependent positive inotropic effect (PIE) should be observed only in the presence of the physiological buffer. Consistently, no effect of KH7 was

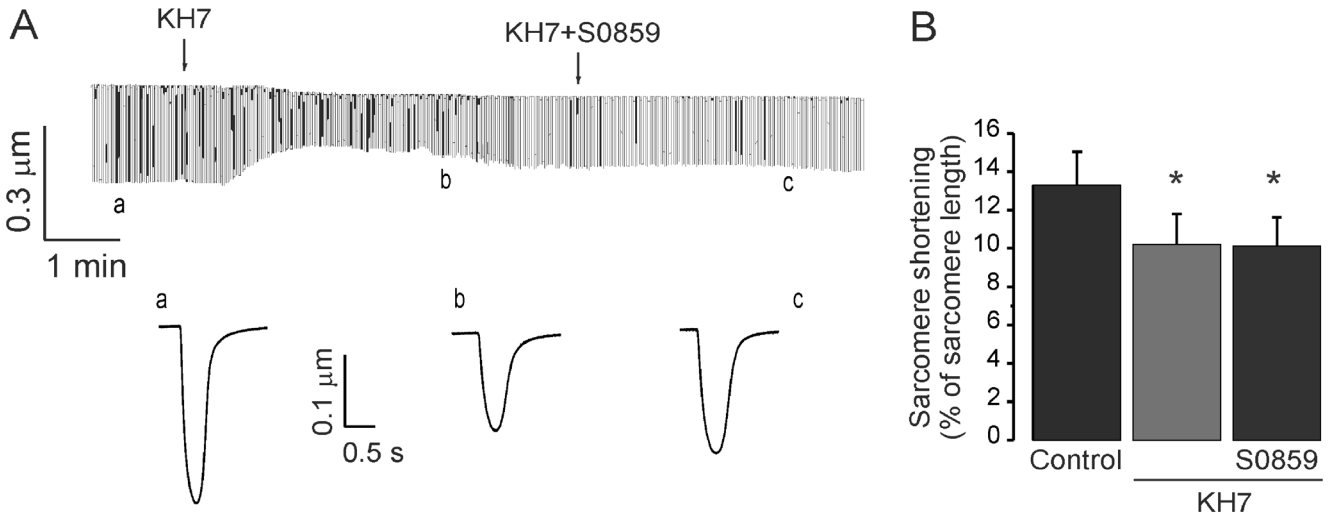

Fig. 1 Participation of sAC in basal cardiac contractility. **A** (upper panel) Representative continuous recordings of sarcomere shortening in the presence of extracellular HCO_3^- before and after the addition of the sAC specific inhibitor KH7 (1 μM) and KH7 plus S0859 (10 μM). **A** (lower panel) Individual traces of sarcomere shortening corresponding to the points indicated in the upper panel as a, b, and c. **B** Average data of sarcomere shortening obtained under the experimental conditions described in **a** ($n = 9$). *$p < 0.05$ vs. control

detected in the absence of extracellular HCO_3^- (HEPES-buffered solution; Fig. 2A). Moreover, it has been demonstrated that the major entry of HCO_3^- into the cardiomyocyte is the NBC. The NBC is an alkalinizing mechanism, which is responsible for 30% of the recovery from acidosis during an *ammonium pulse* and 50% of the maintenance of basal intracellular pH (pH_i). To evaluate if the NBC-mediated HCO_3^- influx is stimulating sAC activity and contributing to the regulation of basal cardiac contractility, we pre-incubated the myocytes during 10 min with the selective NBC blocker, S0859 (10 μM). Figure 3 shows that in the presence of S0859 the cells exhibit a 20% NIE, suggesting that the NBC contributes to basal cardiac contractility. Moreover, when S0859 was added to the cells pre-incubated with KH7, they did not manifest an additional NIE (Fig. 1), suggesting that the activity of sAC and NBC is involved in the same pathway that regulates basal cardiac contractility. It is important to note that, as expected, no effect of S0859 was observed in the absence of HCO_3^- (Fig. 2B).

The hypothesis that HCO_3^--dependent sAC activity is contributing to basal contractility would entail that basal cell shortening should be greater in the presence of HCO_3^- than in its absence. Consistently, in experiments in which we exposed the myocytes to the switching from HEPES- to HCO_3^--buffered extracellular solutions, we detected that the steady-state cell shortening was significantly higher in the presence of the physiological buffer (22.31 ± 1.42%) than in its absence (19.61 ± 1.79%, $n = 7$; $p < 0.01$).

We next tested if S0859 has any influence in pH_i and, as a consequence, in cell shortening. The myocytes were loaded with BCECF, a pH_i indicator, and the sarcomere shortening was measured simultaneously with pH_i. Importantly, while exerting the NIE, S0859 did not affect pH_i (Fig. 4; pH_i after 10 min of S0859 treatment: control: 7.19 ± 0.02, S0859: 7.15 ± 0.02; $n = 6$).

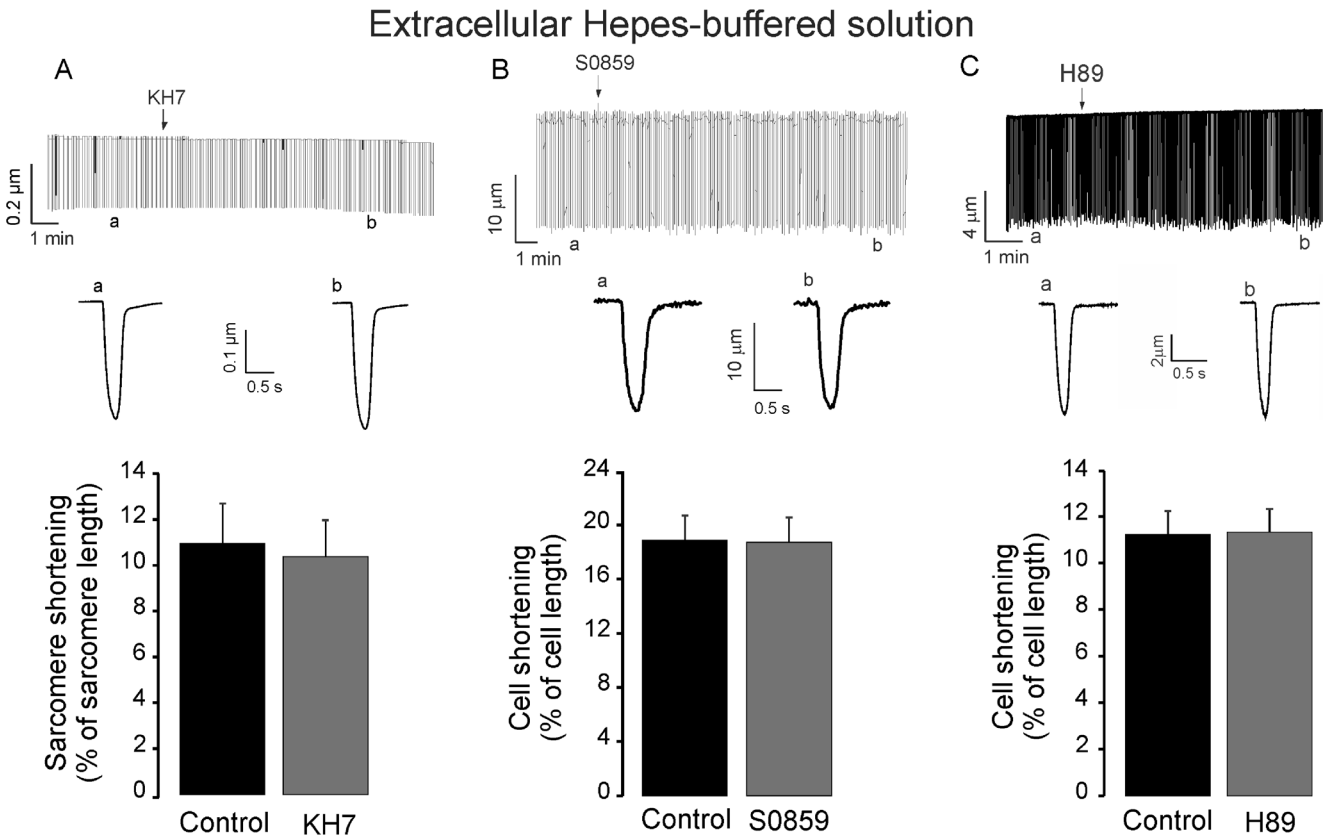

Fig. 2 Basal cardiac contractility in the absence of extracellular HCO_3^-. **A** (upper panel) Representative continuous recordings of sarcomere shortening in the absence of extracellular HCO_3^- (HEPES-buffered solution) before and after the addition of the sAC specific inhibitor KH7 (1 μM). **A** (middle panel) Individual traces of sarcomere shortening corresponding to the points indicated in the upper panel as a and b. **A** (lower panel) Average data of sarcomere shortening obtained under the experimental conditions described in the upper panel ($n = 9$). **B** (upper panel) Representative continuous recordings of cell shortening in the absence of extracellular HCO_3^- (HEPES-buffered solution) before and after the addition of the NBC selective blocker S0859 (10 μM). **B** (middle panel) Individual traces of cell shortening corresponding to the points indicated in the upper panel as a and b. **B** (lower panel) Average data of cell shortening obtained under the experimental conditions described in the upper panel ($n = 9$). **C** (upper panel) Representative continuous recordings of cell shortening in the absence of extracellular HCO_3^- (HEPES-buffered solution) before and after the addition of the PKA selective blocker H89 (0.1 μM). **C** (middle panel) Individual traces of cell shortening corresponding to the points indicated in the upper panel as a and b. **C** (lower panel) Average data of cell shortening obtained under the experimental conditions described in the upper panel ($n = 10$)

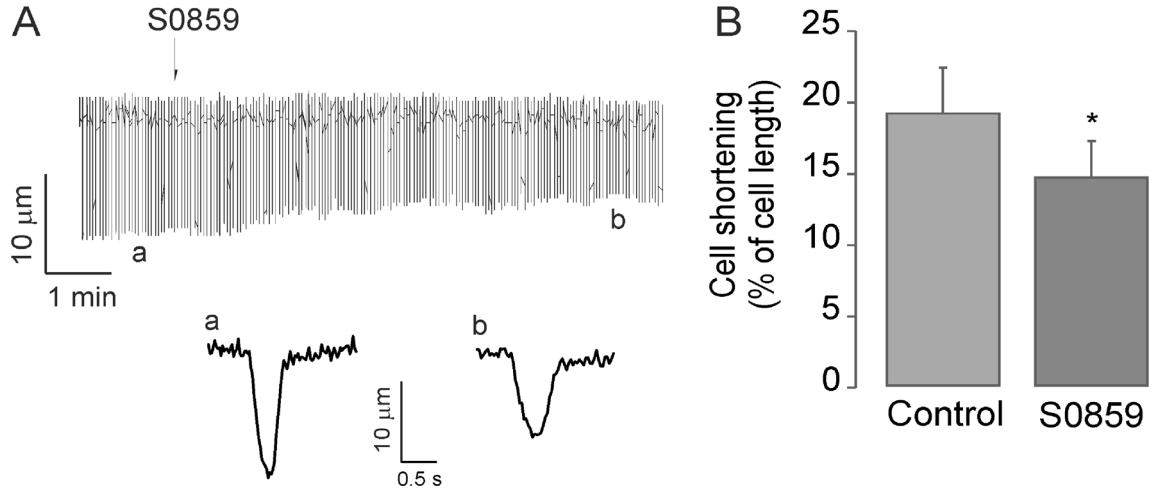

Fig. 3 Participation of NBC in basal cardiac contractility. **A** (upper panel) Representative continuous recordings of cell shortening in the presence of extracellular HCO_3^- before and after the addition of the NBC selective blocker S0859 (10 μM). **A** (lower panel) Individual traces of cell shortening corresponding to the points indicated in the upper panel as a and b. **B** Average data of cell shortening obtained under the experimental conditions described for **A** ($n = 9$). *$p < 0.05$ vs. control

Role of PKA in basal cardiac contractility

In order to keep elucidating the signaling pathway involved in the regulation of basal cardiac contractility, we evaluated the role of PKA. The myocytes were pre-incubated with the PKA blocker H89 (0.1 μM) and cell shortening was evaluated. As shown in Fig. 5, when the myocytes were exposed to H89, they exhibited a reduction in cell shortening of approximately 20%. Moreover, when KH7 is added to the solution already containing H89, the cells did not exert further NIE. These results indicate that PKA activation is involved in the NBC-sAC pathway. It is important to note that this dose of H89 did not affect basal contractility in the absence of extracellular HCO_3^- (Fig. 2C), suggesting the activation of PKA by cAMP produced by sAC, which is HCO_3^--dependent.

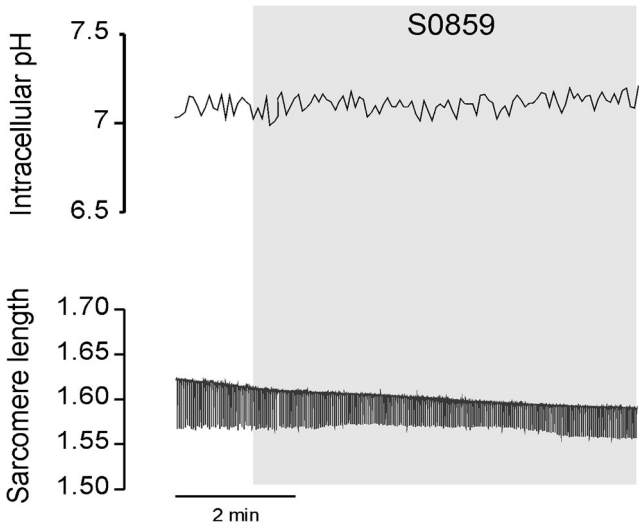

Fig. 4 NBC blockade does not affect resting pH_i. Representative continuous recordings of intracellular pH (pH_i) (upper panel) and sarcomere shortening (lower panel) registered simultaneously, in the presence of extracellular HCO_3^-, and before and after the addition of the NBC blocker S0859 (10 μM, gray-shaded area)

Role of NBC and sAC in calcium transient

To establish if the effect of the NBC-sAC pathway on the contractile response is due to changes in Ca^{2+} handling, we loaded the myocytes with a fluorescent Ca^{2+} indicator (Fura-2, AM) and measured Ca^{2+} transients in myocytes pre-incubated with S0859, KH7, or H89. Figure 6 depicts that S0859, KH7, or H89 reduced approximately 15–20% the amplitude of Ca^{2+} transient, suggesting that the NIE generated by these drugs is secondary to a reduced availability of Ca^{2+} during systole. Again, the simultaneous employment of KH7 with S0859 or H89 did not result in additional effect compared to that exhibited separately.

Role of sAC in the regulation of the RyR

In the heart, PKA-induced PIE is mainly mediated by phosphorylation of the voltage-dependent Ca^{2+} channel (L_{Ca}) and the SR Ca^{2+} release channels (RyR). Besides, the phosphorylation of PLB allows the SR Ca^{2+} pump (SERCA-2A) to introduce more Ca^{2+} into the SR, increasing the Ca^{2+} load and its availability to be used in the following contraction. To investigate the role of NBC-sAC pathway in RyR activity, we recorded Ca^{2+} sparks as an index of RyR ability to increase cytosolic Ca^{2+} through cells loaded with Fluo-3. Two consecutive trains of stimulus of 0.5 Hz were applied to the same cell, being the quiescent period after the first one the control and the second one the time-control or the one treated with KH7 (protocol scheme in Fig. 7A). Although the amplitude of the sparks did not change (Fig. 7D), the occurrence of Ca^{2+} sparks significantly diminished after the inhibition of sAC (Fig. 7C). These

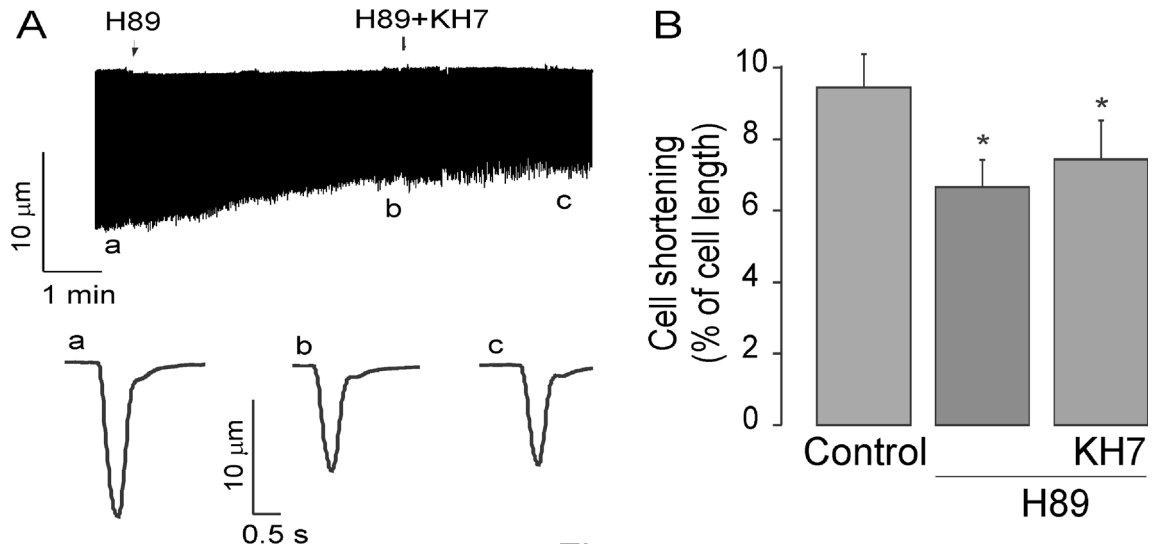

Fig. 5 Participation of PKA in basal cardiac contractility. **A** (upper panel) Representative continuous recordings of cell shortening in the presence of extracellular HCO_3^- before and after the addition of the PKA inhibitor H89 (0.1 μM) and H89 plus KH7 (1 μM). **A** (lower panel) Individual traces of cell shortening corresponding to the points indicated in the upper panel as a, b, and c. **B** Average data of cell shortening obtained under the experimental conditions described in **A** (n = 12). *p < 0.05 vs. control

results demonstrate that sAC is important to regulate RyR activity, probably dependent on PKA phosphorylation. However, the changes in Ca^{2+} spark properties are not necessarily due to direct effects on RyR. Indeed, Fig. 8 shows that the treatment of the myocytes with the sAC inhibitor KH7 reduced the SR Ca^{2+} load, effect that can explain, at least in part, the decreased Ca^{2+} sparks frequency observed with this inhibitor. Consistent with the diminished SR Ca^{2+} load, the decays of Ca^{2+} transients (time to 50% of relaxation) were slower in the presence of KH7 (0.44 ± 0.06 s) than in its absence (0.37 ± 0.04 s, n = 9; p < 0.05), suggesting that the SERCA-2A-mediated SR Ca^{2+} uptake is depressed when sAC is inactive.

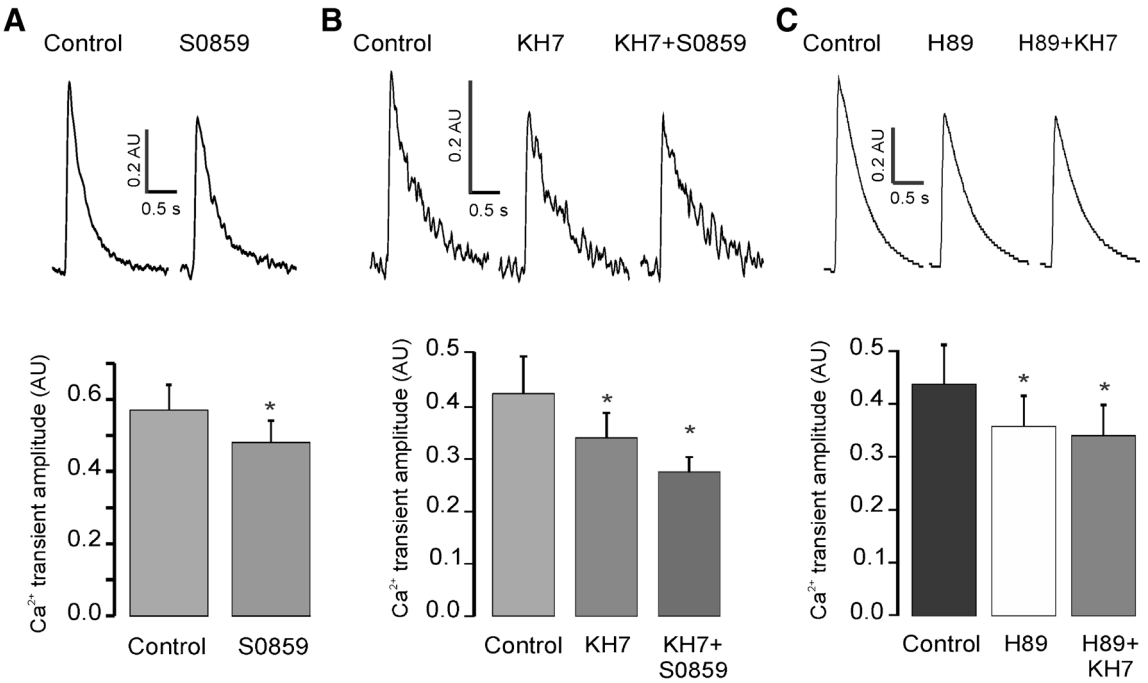

Fig. 6 Effect of NBC, sAC, and PKA blockers on Ca^{2+}_i. **A** Representative individual recordings (upper panel) and average data (lower panel, n = 6) of Ca^{2+}_i before and after the addition of S0859 (10 μM). **B** Representative individual recordings (upper panel) and average data (lower panel, n = 9) of Ca^{2+}_i before and after the addition of KH7 (1 μM) and KH7 plus S0859 (10 μM). **C** Representative individual recordings (upper panel) and average data (lower panel, n = 9) of Ca^{2+}_i before and after the addition of H89 (0.1 μM) and H89 plus KH7 (1 μM). *p < 0.05 vs. control

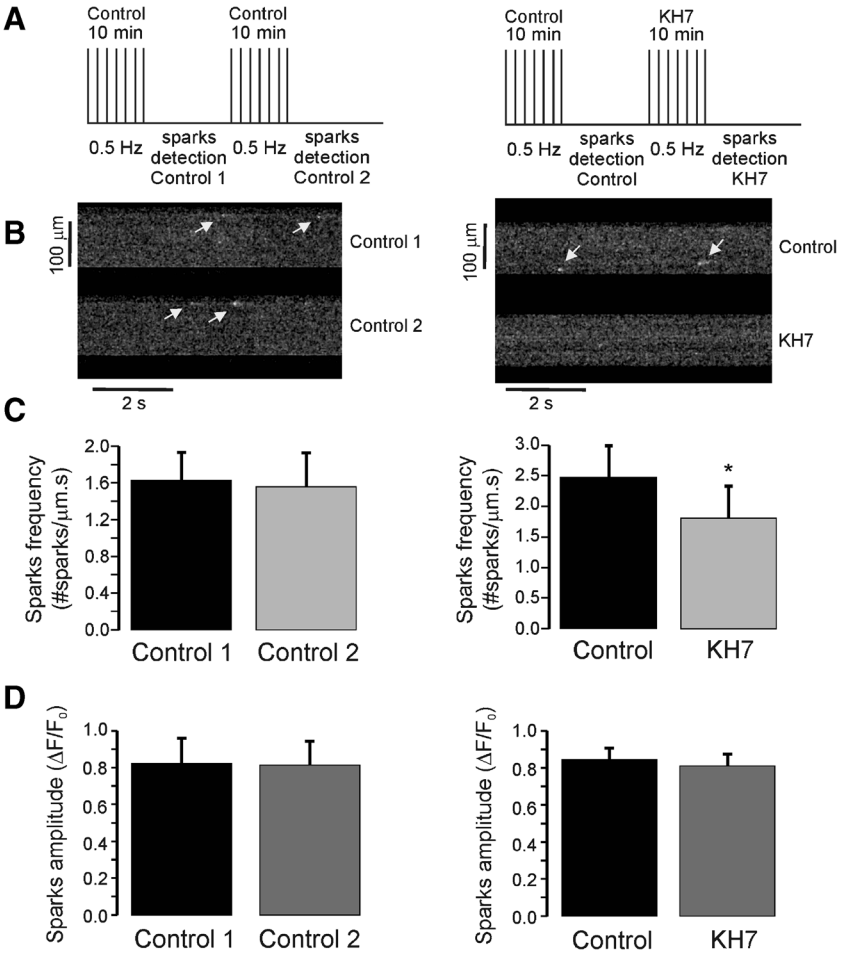

Fig. 7 Effects of sAC blocker on Ca^{2+} sparks frequency. **A** Protocol scheme, two consecutive trains of stimulus of 0.5 Hz for 10 min were applied to the same cell. During the first quiescent period, control sparks were counted and in the second one the occurrence of sparks were counted as time-control (Control 2) or after KH7 treatment. **B** Representative images of Ca^{2+} recorded sparks after each train of stimulus. On the left panel, the control situation; at the upper part, a line scan image after first train of stimulus; at the bottom, an image after a second train of stimulus. On the right panel, the KH7-treated situation; at the upper part, a line scan image after first train of stimulus; and at the bottom, the one after a second train of stimulus during KH7 incubation. **C** Average Ca^{2+} sparks frequency (number of Ca^{2+} sparks/seconds × micrometers of the cell recorded) estimated from confocal microscopy line scan photographs of quiescent myocytes obtained immediately after paced them, in time-control (left panel **C**, $n = 6$) or KH7 incubation (right panel **C**, $n = 6$). **D** Average Ca^{2+} sparks amplitude in the time-control or KH7 treatment, at left or at right panels, respectively. This parameter was estimated from the same quiescence periods where the sparks were counted (see protocols in the upper panels) *$p < 0.05$ vs. control

Role of sAC in the regulation of NBC

Finally, we investigated the potential role of sAC activation on NBC activity. We performed ammonium pulses in BCECF-loaded myocytes and we studied the recovery from acidosis in HCO_3^--containing solution plus the continuous presence of the NHE inhibitor HOE642 (cariporide). Two consecutive ammonium pulses were assessed, being the first one the control and the second one the treatment with KH7 or H89. As depicted in Fig. 9, the NBC-mediated recovery from acidosis was faster in the presence of each compound, suggesting that the pathway sAC-PKA is negatively regulating NBC function, consistent with a negative feedback modulation of the HCO_3^- influx that activates sAC.

sAC is present in the cytosolic extract

Although sAC has been previously detected in cardiac myocytes [2, 33, 45], the exact localization of this enzyme in the cell has not been clearly determined. Since in one of these studies sAC was described at mitochondrial localization [45] and cAMP cannot pass through the mitochondrial inner membrane [1], our results would necessarily implicate a cAMP production by a sAC located at the cytosol. Thus, we obtained the cytosolic extract from the heart (as it was described in subcellular fractioning and western blotting in the methods section) and performed western blot experiments. Figure 10 shows that we indeed identified sAC in the cytosolic extract, testing its purity with the presence of the cytosolic protein GAPDH and the absence of the mitochondrial channel

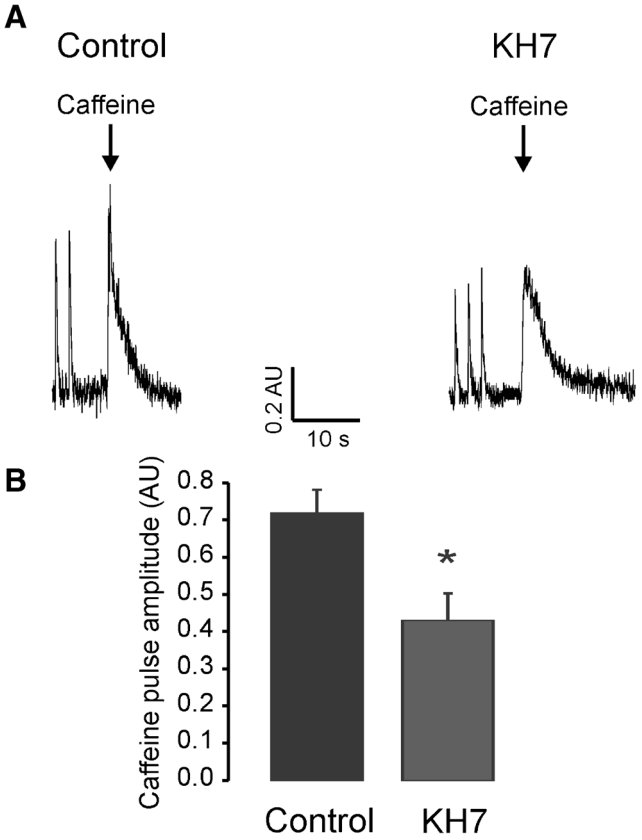

Fig. 8 Effect of sAC inhibitor in SR Ca^{2+} content. **A** Representative records of caffeine pulse after 10 min of 0.5 Hz stimulation, in control situation (left panel) and after KH7 incubation (right panel). **B** Average amplitude of the SR Ca^{2+} release generated in response to the caffeine pulse in Control ($n = 9$) or KH7 ($n = 7$), estimated by Fura-2 ratio (UA). *$p < 0.05$ vs. control

VDAC. As a positive control, we used testis homogenate, a well-known source of sAC. The presence of this enzyme in the cytosolic extract can explain the functional results obtained herein and in recent reports describing the actions of sAC in the cardiovascular system [29, 33].

Discussion

In this study, we demonstrated for the first time the presence of a functional complex formed by NBC and sAC, which participates in the regulation of cardiac basal contractility (Fig. 11). It has been reported that sAC activity depends on HCO_3^- and Ca^{2+} [11, 23, 24, 26]. Based on the knowledge that the major entry of HCO_3^- in cardiac myocytes is mediated by the NBC, we tested whether sAC activity is dependent on such transporter. Our findings, using S0859, the specific inhibitor of NBC, strongly support our hypothesis that NBC delivers to sAC the HCO_3^- needed for its activation (Fig. 11). Furthermore, we have also demonstrated the presence of a negative feedback for this NBC-mediated HCO_3^- influx, since we determined a sAC- and PKA-dependent inhibition of NBC activity (Fig. 11). Accordingly, a similar effect of PKA on NBCn1 expressed in a heterologous system has been previously described [27].

Although sAC has been reported to be present in the heart, evidence about its physiological or pathophysiological implications is scarce [10]. It has been previously suggested that following myocardial ischemia, sAC-generated cAMP activates PKA and the pro-apoptotic Bcl-2 pathway, leading to ischemic injury [2]. However, recently and in the opposite direction, a protective role for sAC against cell death, apoptosis as well as necrosis in primary cardiomyocytes has been reported [45]. In this case, a truncated form of soluble sAC (sACt) and the exchange protein directly activated by cAMP 1 (Epac1) seem to be implicated [45]. In addition, an interesting role for sAC in the regulation of the heart rate of the Pacific hagfish, a species that lacks any cardiac innervation, has been recently reported [47]. Moreover, a positive role of sAC in cardiac hypertrophic growth induced by isoprenaline or transverse aortic constriction was demonstrated [33].

In the present study, using different blockers, we demonstrated that the pathway NBC-sAC-PKA regulates basal cardiac contractility, probably due to the activation of RyR by PKA phosphorylation (Fig. 11). The RyR activity was evaluated by the measurement of *Ca^{2+} sparks*, a protocol that estimates the RyR ability to be opened. The assessment of the phosphorylation of the PKA consensus sites of this channel is required to confirm this hypothesis. At the same time, the potential phosphorylation of Ser-16 of phospholamban with the consequent enhancement of SR Ca^{2+} uptake by SERCA-2A is also needed to be performed. Consistently, herein we observed that the Ca^{2+} transient decay is slower and the Ca^{2+} store size is smaller in the presence of the sAC inhibitor than in its absence. Another potential target of PKA that deserves to be analyzed is the L-type Ca^{2+} channel (Ca_L) (Fig. 11). However, although many PKA targets involved in ECC could be considered, it is possible that the NBC-sAC-PKA pathway could only be able to act on a single one. Moreover, sAC represents an alternative source of cAMP that is not limited to the plasma membrane; therefore, it could form discrete signaling microdomains with selective intracellular effectors [51]. Nevertheless, the necessity of performing more experiments to elucidate the complete signaling pathway that links the activation of sAC with the modulation of basal cardiac contractility is recognized.

We described in the present study that the presence of HCO_3^- in the extracellular solution is mandatory to observe the effects of S0859, KH7, and H89, suggesting the involvement of the functional complex NBC-sAC-PKA in physiological ECC. Considering that HCO_3^- represents the main physiological buffer, the data presented herein calls the attention about the assessment of basal cardiac contractility with extracellular solutions without HCO_3^-. Higher levels of contractility in the presence of the physiological buffer were shown in

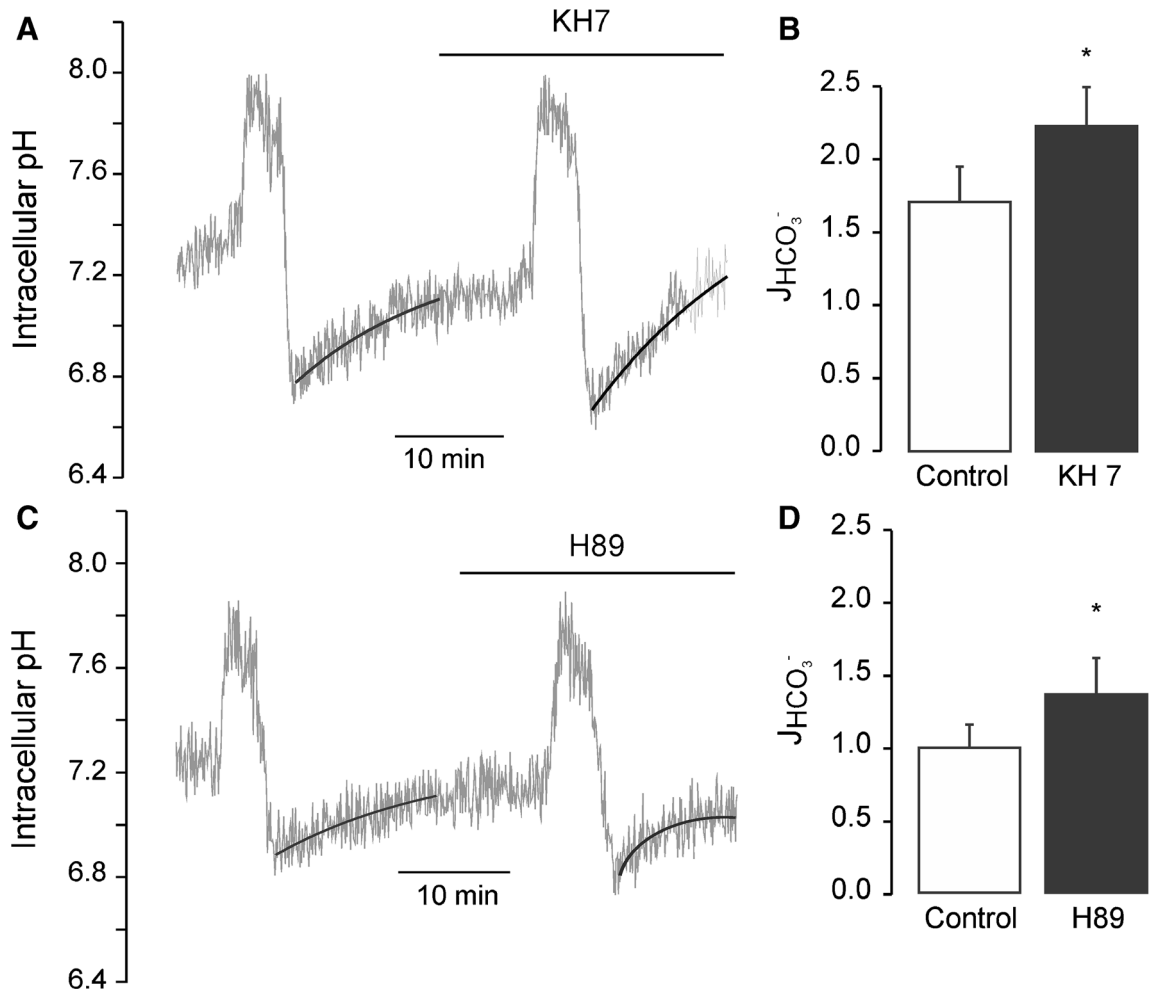

Fig. 9 Effect of sAC and PKA blockers on NBC activity. **A**, **C** Representative traces of pH_i during the application of two consecutive NH_4Cl pulses (20 mM NH_4Cl), in the absence (first pulses) or presence (second pulses) of 1 μM KH7 (**A**) or 0.1 μM H89 (**C**). **B**, **D** Average bicarbonate influx (J_{HCO3-}), carried by NBC at pH_i 6.8, in the absence (Controls) or presence of KH7 (**B**, $n = 8$) or H89 (**D**, $n = 7$). *$p < 0.05$ vs. control

the present work and have been previously reported when cardiac preparations were exposed to switching extracellular solutions from HEPES to HCO_3^- [9, 42, 43]. Since changes in pH_i can alter contractility, one explanation for the S0859-induced NIE could be the possible intracellular acidification produced by the NBC inhibition. However, under our experimental conditions, we did not observe changes in basal pH_i after the treatment with the NBC blocker. At resting pH_i, the proton efflux that maintains the steady state is very low and it is likely that the inhibition of one of the alkalinizing

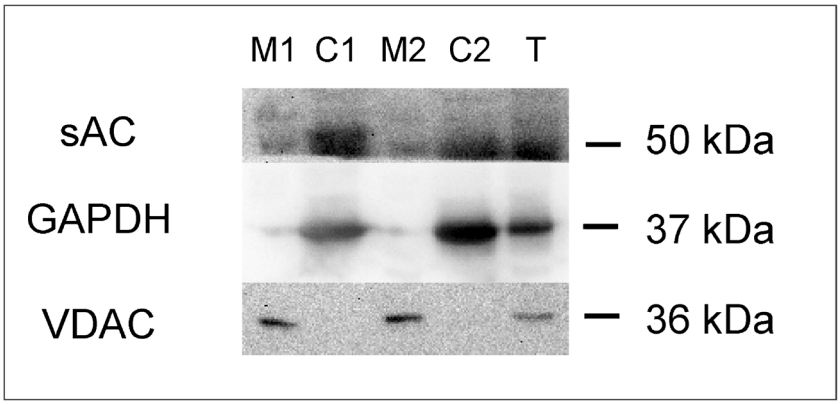

Fig. 10 Presence of sAC in the cytosolic extract. Western blot showing the expression of sAC, GAPDH, and VDAC in samples of mitochondrial fraction (M1 and M2) and cytosolic fraction (C1 and C2). A testis homogenate (T) was used as positive control of all the proteins detected

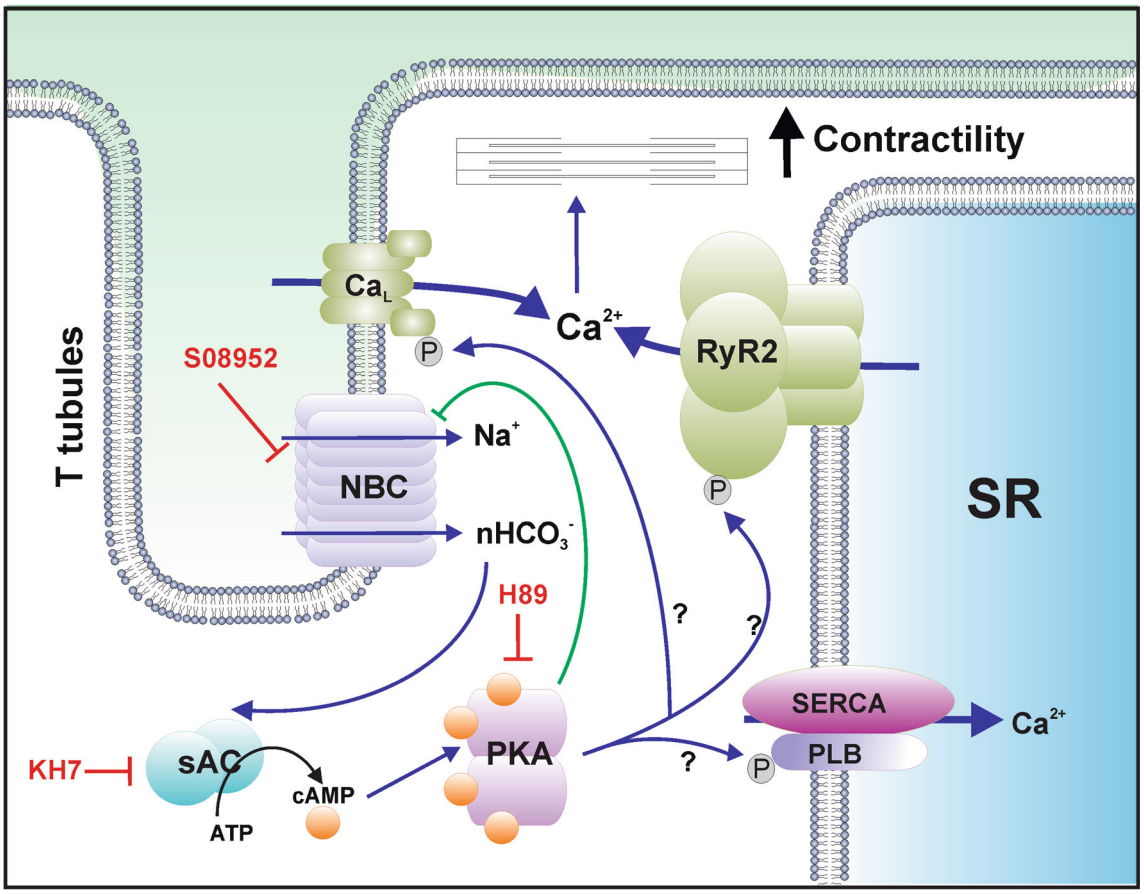

Fig. 11 Hypothesis of the physiological role of sAC in the cardiomyocyte. The NBC-induced bicarbonate influx stimulates sAC which in turn generates the cAMP that activates PKA. This kinase might phosphorylate RyR2 and enhance the release of Ca^{2+} to the cytosol, leading to the increase in contractility. In addition, PKA could stimulate the SR Ca^{2+} re-uptake secondary to phospholamban (PLB) phosphorylation and/or the influx of Ca^{2+} to the cell by phosphorylation of the L-type Ca^{2+} channel (Ca_L). Finally, we propose a PKA-induced inhibition of NBC, limiting the influx of bicarbonate and regulating the whole mechanism with a negative feedback

transporters (NHE or NBC) could be functionally compensated by the one that remains active. Consistently, in the presence of bicarbonate, individual blockade of the NHE [25] or the NBC [30] does not seem to affect resting pH_i.

While NHE is confined to the intercalated disks, NBC is preferentially contained along the T tubules [16]. This localization allows the speculation about the participation of NBC in ECC due to potential interactions with its main protagonists, Ca_L and RyR, which are also confined to the same area [50]. The Na^+/Ca^{2+} exchanger (NCX), another important protein involved in ECC, is also mainly expressed in T tubules [14]. Although in the present study we propose that NBC participates in the maintenance of basal contractility by inducing the influx of HCO_3^-, which in turn activates cAMP generation by sAC, we cannot discard the possibility that the simultaneous Na^+ loading produced by NBC might contribute to the increase in Ca^{2+}_i secondary to the modification of NCX activity. Nevertheless, although we acknowledge that many steps of the myocardial NBC-sAC-PKA pathways remain to be studied, we would like to remark that the results of the present work bring new insights into basic cardiac physiology, by introducing a novel role for an evolutionary conserved enzyme in the control of basal cardiac contractility.

Funding informationThis study was partly supported by grants PICT2014 2594 and PICT2017 1567, and PIP 0725 of the Agencia Nacional de Promoción Científica y Tecnológica de Argentina (ANCPyT) and of the Consejo Nacional de Investigaciones Científicas y Técnicas (CONICET), respectively.

Compliance with ethical standards

Conflict of interest The authors declare that they have no conflict of interest.

References

1. Acin-Perez R, Salazar E, Kamenetsky M, Buck J, Levin LR, Manfredi G (2009) Cyclic AMP produced inside mitochondria regulates oxidative phosphorylation. Cell Metab 9:265–276. https://doi.org/10.1016/j.cmet.2009.01.012

2. Appukuttan A, Kasseckert SA, Micoogullari M, Flacke JP, Kumar S, Woste A, Abdallah Y, Pott L, Reusch HP, Ladilov Y (2012) Type 10 adenylyl cyclase mediates mitochondrial Bax translocation and apoptosis of adult rat cardiomyocytes under simulated ischaemia/reperfusion. Cardiovasc Res 93:340–349. https://doi.org/10.1093/cvr/cvr306
3. Baudouin-Legros M, Hamdaoui N, Borot F, Fritsch J, Ollero M, Planelles G, Edelman A (2008) Control of basal CFTR gene expression by bicarbonate-sensitive adenylyl cyclase in human pulmonary cells. Cell Physiol Biochem 21:75–86. https://doi.org/10.1159/000113749
4. Bers DM (2006) Cardiac ryanodine receptor phosphorylation: target sites and functional consequences. Biochem J 396:e1–e3. https://doi.org/10.1042/BJ20060377
5. Biel M (2009) Cyclic nucleotide-regulated cation channels. J Biol Chem 284:9017–9021. https://doi.org/10.1074/jbc.R800075200
6. Bitterman JL, Ramos-Espiritu L, Diaz A, Levin LR, Buck J (2013) Pharmacological distinction between soluble and transmembrane adenylyl cyclases. J Pharmacol Exp Ther 347:589–598. https://doi.org/10.1124/jpet.113.208496
7. Braun T, Dods RF (1975) Development of a Mn^{2+}-sensitive, "soluble" adenylate cyclase in rat testis. Proc Natl Acad Sci U S A 72:1097–1101
8. Buck J, Sinclair ML, Schapal L, Cann MJ, Levin LR (1999) Cytosolic adenylyl cyclase defines a unique signaling molecule in mammals. Proc Natl Acad Sci U S A 96:79–84
9. Camilion de Hurtado MC, Perez NG, Cingolani HE (1995) An electrogenic sodium-bicarbonate cotransport in the regulation of myocardial intracellular pH. J Mol Cell Cardiol 27:231–242
10. Chen J, Levin LR, Buck J (2012) Role of soluble adenylyl cyclase in the heart. Am J Physiol Heart Circ Physiol 302:H538–H543. https://doi.org/10.1152/ajpheart.00701.2011
11. Chen Y, Cann MJ, Litvin TN, Iourgenko V, Sinclair ML, Levin LR, Buck J (2000) Soluble adenylyl cyclase as an evolutionarily conserved bicarbonate sensor. Science 289:625–628
12. De Giusti VC, Orlowski A, Ciancio MC, Espejo MS, Gonano LA, Caldiz CI, Vila Petroff MG, Villa-Abrille MC, Aiello EA (2015) Aldosterone stimulates the cardiac sodium/bicarbonate cotransporter via activation of the g protein-coupled receptor gpr30. J Mol Cell Cardiol 89:260–267. https://doi.org/10.1016/j.yjmcc.2015.10.024
13. De Giusti VC, Orlowski A, Villa-Abrille MC, de Cingolani GE, Casey JR, Alvarez BV, Aiello EA (2011) Antibodies against the cardiac sodium/bicarbonate co-transporter (NBCe1) as pharmacological tools. Br J Pharmacol 164:1976–1989
14. Despa S, Brette F, Orchard CH, Bers DM (2003) Na/Ca exchange and Na/K-ATPase function are equally concentrated in transverse tubules of rat ventricular myocytes. Biophys J 85:3388–3396. https://doi.org/10.1016/S0006-3495(03)74758-4
15. Fujita T, Umemura M, Yokoyama U, Okumura S, Ishikawa Y (2017) The role of Epac in the heart. Cell Mol Life Sci 74:591–606. https://doi.org/10.1007/s00018-016-2336-5
16. Garciarena CD, Ma YL, Swietach P, Huc L, Vaughan-Jones RD (2013) Sarcolemmal localisation of Na^+/H^+ exchange and Na^+-HCO_3^- co-transport influences the spatial regulation of intracellular pH in rat ventricular myocytes. J Physiol 591:2287–2306
17. Gautel M, Zuffardi O, Freiburg A, Labeit S (1995) Phosphorylation switches specific for the cardiac isoform of myosin binding protein-C: a modulator of cardiac contraction? EMBO J 14:1952–1960
18. Geng W, Hill K, Zerwekh JE, Kohler T, Muller R, Moe OW (2009) Inhibition of osteoclast formation and function by bicarbonate: role of soluble adenylyl cyclase. J Cell Physiol 220:332–340. https://doi.org/10.1002/jcp.21767
19. Hagemann D, Xiao RP (2002) Dual site phospholamban phosphorylation and its physiological relevance in the heart. Trends Cardiovasc Med 12:51–56
20. Halm ST, Zhang J, Halm DR (2010) beta-Adrenergic activation of electrogenic K^+ and Cl^- secretion in guinea pig distal colonic epithelium proceeds via separate cAMP signaling pathways. Am J Physiol Gastrointest Liver Physiol 299:G81–G95. https://doi.org/10.1152/ajpgi.00035.2010
21. Hallows KR, Wang H, Edinger RS, Butterworth MB, Oyster NM, Li H, Buck J, Levin LR, Johnson JP, Pastor-Soler NM (2009) Regulation of epithelial Na^+ transport by soluble adenylyl cyclase in kidney collecting duct cells. J Biol Chem 284:5774–5783. https://doi.org/10.1074/jbc.M805501200
22. Imber AN, Santin JM, Graham CD, Putnam RW (2014) A HCO_3^--dependent mechanism involving soluble adenylyl cyclase for the activation of Ca^{2+} currents in locus coeruleus neurons. Biochim Biophys Acta 1842:2569–2578. https://doi.org/10.1016/j.bbadis.2014.07.027
23. Jaiswal BS, Conti M (2003) Calcium regulation of the soluble adenylyl cyclase expressed in mammalian spermatozoa. Proc Natl Acad Sci U S A 100:10676–10681. https://doi.org/10.1073/pnas.1831008100
24. Kleinboelting S, Diaz A, Moniot S, van den Heuvel J, Weyand M, Levin LR, Buck J, Steegborn C (2014) Crystal structures of human soluble adenylyl cyclase reveal mechanisms of catalysis and of its activation through bicarbonate. Proc Natl Acad Sci U S A 111:3727–3732. https://doi.org/10.1073/pnas.1322778111
25. Leem CH, Lagadic-Gossmann D, Vaughan-Jones RD (1999) Characterization of intracellular pH regulation in the guinea-pig ventricular myocyte. J Physiol 517(Pt 1):159–180
26. Litvin TN, Kamenetsky M, Zarifyan A, Buck J, Levin LR (2003) Kinetic properties of "soluble" adenylyl cyclase. Synergism between calcium and bicarbonate J Biol Chem 278:15922–15926. https://doi.org/10.1074/jbc.M212475200
27. Loiselle FB, Morgan PE, Alvarez BV, Casey JR (2004) Regulation of the human NBC3 Na^+/HCO_3^- cotransporter by carbonic anhydrase II and PKA. Am J Phys Cell Phys 286:C1423–C1433. https://doi.org/10.1152/ajpcell.00382.2003
28. Orlowski A, Ciancio MC, Caldiz CI, De Giusti VC, Aiello EA (2014) Reduced sarcolemmal expression and function of the NBCe1 isoform of the Na^+-HCO_3^- cotransporter in hypertrophied cardiomyocytes of spontaneously hypertensive rats: role of the renin-angiotensin system. Cardiovasc Res 101:211–219. https://doi.org/10.1093/cvr/cvt255
29. Parker T, Wang KW, Manning D, Dart C (2019) Soluble adenylyl cyclase links Ca^{2+} entry to Ca^{2+}/cAMP-response element binding protein (CREB) activation in vascular smooth muscle. Sci Rep 9:7317. https://doi.org/10.1038/s41598-019-43821-3
30. Perez NG, Alvarez BV, Camilion de Hurtado MC, Cingolani HE (1995) pH_i regulation in myocardium of the spontaneously hypertensive rat. Compensated enhanced activity of the Na^+-H^+ exchanger. Circ Res 77:1192–1200
31. Picht E, Zima AV, Blatter LA, Bers DM (2007) SparkMaster: automated calcium spark analysis with ImageJ. Am J Phys Cell Phys 293:C1073–C1081. https://doi.org/10.1152/ajpcell.00586.2006
32. Ramos-Espiritu L, Kleinboelting S, Navarrete FA, Alvau A, Visconti PE, Valsecchi F, Starkov A, Manfredi G, Buck H, Adura C, Zippin JH, van den Heuvel J, Glickman JF, Steegborn C, Levin LR, Buck J (2016) Discovery of LRE1 as a specific and allosteric inhibitor of soluble adenylyl cyclase. Nat Chem Biol 12:838–844. https://doi.org/10.1038/nchembio.2151
33. Schirmer I, Bualeong T, Budde H, Cimiotti D, Appukuttan A, Klein N, Steinwascher P, Reusch P, Mugge A, Meyer R, Ladilov Y, Jaquet K (2018) Soluble adenylyl cyclase: a novel player in cardiac hypertrophy induced by isoprenaline or pressure overload. PLoS One 13:e0192322. https://doi.org/10.1371/journal.pone.0192322
34. Schmid A, Sutto Z, Nlend MC, Horvath G, Schmid N, Buck J, Levin LR, Conner GE, Fregien N, Salathe M (2007) Soluble adenylyl cyclase is localized to cilia and contributes to ciliary beat

frequency regulation via production of cAMP. J Gen Physiol 130: 99–109. https://doi.org/10.1085/jgp.200709784
35. Steegborn C, Litvin TN, Levin LR, Buck J, Wu H (2005) Bicarbonate activation of adenylyl cyclase via promotion of catalytic active site closure and metal recruitment. Nat Struct Mol Biol 12:32–37. https://doi.org/10.1038/nsmb880
36. Strang KT, Sweitzer NK, Greaser ML, Moss RL (1994) Beta-adrenergic receptor stimulation increases unloaded shortening velocity of skinned single ventricular myocytes from rats. Circ Res 74:542–549
37. Sun XC, Zhai CB, Cui M, Chen Y, Levin LR, Buck J, Bonanno JA (2003) HCO_3^--dependent soluble adenylyl cyclase activates cystic fibrosis transmembrane conductance regulator in corneal endothelium. Am J Phys Cell Phys 284:C1114–C1122. https://doi.org/10.1152/ajpcell.00400.2002
38. Tresguerres M, Levin LR, Buck J (2011) Intracellular cAMP signaling by soluble adenylyl cyclase. Kidney Int 79:1277–1288. https://doi.org/10.1038/ki.2011.95
39. Tresguerres M, Levin LR, Buck J, Grosell M (2010) Modulation of NaCl absorption by [HCO_3^-] in the marine teleost intestine is mediated by soluble adenylyl cyclase. Am J Phys Regul Integr Comp Phys 299:R62–R71. https://doi.org/10.1152/ajpregu.00761.2009
40. Vaughan-Jones RD, Spitzer KW, Swietach P (2009) Intracellular pH regulation in heart. J Mol Cell Cardiol 46:318–331
41. Vaughan-Jones RD, Villafuerte FC, Swietach P, Yamamoto T, Rossini A, Spitzer KW (2006) pH-Regulated Na^+ influx into the mammalian ventricular myocyte: the relative role of Na^+-H^+ exchange and Na^+-HCO_3^- co-transport. J Cardiovasc Electrophysiol 17(Suppl 1):S134–S140
42. Villa-Abrille MC, Petroff MG, Aiello EA (2007) The electrogenic Na^+/HCO_3^- cotransport modulates resting membrane potential and action potential duration in cat ventricular myocytes. J Physiol 578: 819–829. https://doi.org/10.1113/jphysiol.2006.120170
43. Wang HS, Chen Y, Vairamani K, Shull GE (2014) Critical role of bicarbonate and bicarbonate transporters in cardiac function. World J Biol Chem 5:334–345. https://doi.org/10.4331/wjbc.v5.i3.334
44. Wang Y, Lam CS, Wu F, Wang W, Duan Y, Huang P (2005) Regulation of CFTR channels by HCO_3^--sensitive soluble adenylyl cyclase in human airway epithelial cells. Am J Phys Cell Phys 289: C1145–C1151. https://doi.org/10.1152/ajpcell.00627.2004
45. Wang Z, Liu D, Varin A, Nicolas V, Courilleau D, Mateo P, Caubere C, Rouet P, Gomez AM, Vandecasteele G, Fischmeister R, Brenner C (2016) A cardiac mitochondrial cAMP signaling pathway regulates calcium accumulation, permeability transition and cell death. Cell Death Dis 7:e2198. https://doi.org/10.1038/cddis.2016.106
46. Weiss S, Oz S, Benmocha A, Dascal N (2013) Regulation of cardiac L-type Ca^{2+} channel CaV1.2 via the beta-adrenergic-cAMP-protein kinase A pathway: old dogmas, advances, and new uncertainties. Circ Res 113:617–631. https://doi.org/10.1161/CIRCRESAHA.113.301781
47. Wilson CM, Roa JN, Cox GK, Tresguerres M, Farrell AP (2016) Introducing a novel mechanism to control heart rate in the ancestral Pacific hagfish. J Exp Biol 219:3227–3236. https://doi.org/10.1242/jeb.138198
48. Yamamoto T, Shirayama T, Sakatani T, Takahashi T, Tanaka H, Takamatsu T, Spitzer KW, Matsubara H (2007) Enhanced activity of ventricular Na^+-HCO_3^- cotransport in pressure overload hypertrophy. Am J Physiol Heart Circ Physiol 293:H1254–H1264
49. Yamamoto T, Swietach P, Rossini A, Loh SH, Vaughan-Jones RD, Spitzer KW (2005) Functional diversity of electrogenic Na^+-HCO_3^- cotransport in ventricular myocytes from rat, rabbit and guinea pig. J Physiol 562:455–475
50. Ziman AP, Gomez-Viquez NL, Bloch RJ, Lederer WJ (2010) Excitation-contraction coupling changes during postnatal cardiac development. J Mol Cell Cardiol 48:379–386. https://doi.org/10.1016/j.yjmcc.2009.09.016
51. Zippin JH, Chen Y, Nahirney P, Kamenetsky M, Wuttke MS, Fischman DA, Levin LR, Buck J (2003) Compartmentalization of bicarbonate-sensitive adenylyl cyclase in distinct signaling microdomains. FASEB J 17:82–84. https://doi.org/10.1096/fj.02-0598fje
52. Zippin JH, Chen Y, Straub SG, Hess KC, Diaz A, Lee D, Tso P, Holz GG, Sharp GW, Levin LR, Buck J (2013) CO_2/HCO_3^-- and calcium-regulated soluble adenylyl cyclase as a physiological ATP sensor. J Biol Chem 288:33283–33291. https://doi.org/10.1074/jbc.M113.510073